Supplementary Material

High-performance Low Temperature Curable Copolyimides via Multidimensional Modulation in Alkaline and Electronic Effects of Monomers

Xialei Lv§[a], Shan Huang§[a, b], Zimeng He[a], Jinhui Li*[a], Siyao Qiu[a], Tao Wang[a], Yun Bai[a], Yao Zhang[a], Guoping Zhang*[a], and Rong Sun[a]

[a] Shenzhen International Innovation Institutes of Advanced Electronic Materials, Shenzhen Institutes of Advanced Technology, Chinese Academy of Sciences, Shenzhen 518055, China.

[b] Department of Nano Science and Technology Institute, University of Science and Technology of China, Suzhou, 215123, China

§These authors contribute equally to this work.

E-mail: jh.li@siat.ac.cn and gp.zhang@siat.ac.cn

Table of Contents

I. Experimental Section

Instruments

The NMR spectra were tested by a Brucker AVANCE III 400 MHz spectrometer (^{1}H NMR: 400 MHz, ^{13}C NMR: 100 MHz) to confirmed the structure of intermediates and end products. The high-performance liquid chromatography (HPLC) was obtained by Ultimate 3000 to estimate the purity of diamine monomer $MePMNH_2$ and $2MePMNH_2$. The Fourier transform-infrared (FT-IR) spectra and polarized attenuated total reflection/Fourier transform infrared spectroscopy were recorded with Vertex 70 (Bruker, Germany) from 4000 cm^{-1} to 600 cm^{-1}. Wide-angle X-ray data were collected on a Bruker D8 Advance diffractometer (Bruker, Germany) with CuKα radiation at a wavelength of 0.15418 nm with step scanning by 2θ intervals from 5° to 50°. The *d*-spacing was calculated according to Bragg's equation: $\lambda = 2d*\sin\theta$. The thermal properties such as T_d (thermal decomposition temperature) were tested using a STD Q600 (TA Instruments, America). Coefficient of thermal expansion (CTE) of the PI films and T_g (glass transition temperature) were measured with thermal mechanical analysis (TMA) with a heating rate of 10°C/min from 30-400°C by NETZSCHTMA 402. The mechanical properties of the samples were also measured using DMA Q800 with a constant stretching speed of 2 N min^{-1} at room temperature. The high frequency dielectric constant (10 GHz) of PI films was measured by e5071c keysight ENA vector network analyzer, and the samples were pretreated in oven at 150°C for 2 h. The cyclic voltammetry curves were recorded on a computer-controlled EG&G Potentiostat/Galvanostat model 283 at room temperature with a conventional three-electrode system, which consisted of a platinum wire counter electrode, a AgCl/Ag

reference electrode, and a Pt carbon working electrode of 2 mm diameter. The supporting electrolyte was 0.1 M tetrabutylammonium hexafluorophosphate (Bu4NPF6) in dry dichloromethane, and ferrocene was added as a calibrant in the whole measurement. Incidentally, most of the general methods are the same as our published paper before.[1]

Calculations

The ground state (S_0) geometries of the three diamines were optimized by density functional theory (DFT) with B3LYP functional 6-31G basis set via Gaussian 16.[2] The pKa values were calculated by B3LYP functional with Def2TZVP basis set.[3] Besides, polarizable continuum model (PCM) with DMAc solvent has been included in pKa calculations.[4] To obtain accurate proton energy under DMAc solvent, proton binding with 7 DMAc molecules have been calculated.[5]

II. Synthesis of monomers.

Synthesis of 4,4'-((5-methylpyrimidine-2,4-diyl)bis(oxy))dianiline ($MePMNH_2$)

Synthesis of $MePMNO_2$. As shown in Scheme S1, 2,4-dichloro-5-methylpyrimidine (12.00 g, 73.5 mmol), *p*-nitrophenol (30.68 g, 220.5 mmol), potassium carbonate (30.48 g, 220.5 mmol), and DMF (50 mL) were successively weighed into a 250 mL three-necked round bottom flask and reacted for 1 h at 150 ℃ under nitrogen. After cooling to room temperature, the reaction solution was extracted with deionized water and dichloromethane. The crude product was collected and purified by chromatography on silica gel with petroleum ether (PE)/dichloromethane (DCM) as an eluent. The purified product was pale-yellow powder with a yield of 85%. ^{1}H NMR, (400 MHz, DMSO-*d6*) δ 8.35 - 8.26 (m, 2H), 8.18 - 8.11 (m, 2H), 8.08 (s, 1H), 7.54 - 7.43 (m, 2H), 7.08 - 6.96 (m, 2H). HRMS (APCI) *m/z*: $[M + H]^+$ calculated for $C_{17}H_{12}O_6N_4$, 369.0811; found,

369.0819.

Synthesis of $MePMNH_2$. The $MePMNO_2$ (15.00 g, 40.7 mmol), 10% Pd/C (0.90 g), and THF (150 mL) were added into a 500 mL three-necked round bottom flask under nitrogen. After heating to reflux with stirring, 10 mL 85% hydrazine hydrate was added dropwise. The solution was followed by refluxing under nitrogen for 16 h. After filtering to remove Pd/C, the crude product was collected and purified by chromatography on silica gel with petroleum ether (PE)/ethyl acetate (EA) as an eluent. The purified product was brown powder with a yield of 80%. ^{1}H NMR, (400 MHz, DMSO-d_6), δ 8.14 (d, J = 0.8 Hz, 1H), 6.85 (d, J = 8.8 Hz, 2H), 6.75 (d, J = 8.8 Hz, 2H), 6.55 (dd, J = 24.9, 8.8 Hz, 4H), 5.05 (s, 2H), 4.98 (s, 2H), 2.15 (s, 3H). ^{13}C NMR (100 MHz, DMSO-d_6) δ 169.92, 164.01, 158.89, 146.77, 146.30, 143.46, 142.64, 127.19, 122.51, 122.21, 114.62, 114.60, 112.22, 12.16. HRMS (APCI) *m/z*: $[M + H]^+$ calculated for $C_{17}H_{16}O_2N_4$, 309.1330; found, 309.1335.

Synthesis of 4,4'-((6-methylpyrimidine-2,4-diyl)bis(oxy))dianiline ($2MePMNH_2$)

Synthesis of $2MePMNO_2$. 2,4-Dichloro-6-methylpyrimidine (12.00 g, 73.5 mmol), *p*-nitrophenol (30.68 g, 220.5 mmol), potassium carbonate (30.48 g, 220.5 mmol), and DMF (50 mL) were weighed into a 250 mL three-necked round bottom flask and reacted for 12 h at 150°C under nitrogen. The crude product was treated in the same way as synthesis of $MePMNO_2$. The purified product was pale-yellow powder with a yield of 81%.^{1}H NMR, (400 MHz, DMSO-d_6), δ 8.44-8.08(m, 4H), 7.67 - 7.35 (m, 4H), 6.97 (s, 1H), 2.41 (s, 3H). HRMS (APCI) *m/z*: $[M + H]^+$ calculated for $C_{17}H_{12}O_6N_4$, 369.0811; found, 369.0816.

Synthesis of $2MePMNH_2$. The $2MePMNO_2$ (15.00 g, 40.7 mmol), 10% Pd/C (0.90 g), and THF (150 mL) were added into a 500 mL 3-neck round bottom flask under nitrogen. After heating to reflux with stirring, 10 mL 85% hydrazine hydrate was added dropwise slowly. The solution was followed by refluxing under nitrogen for only 10 min. The crude product was treated in the same way as synthesis of $MePMNH_2$. The

purified product was white powder with a yield of 85%. ^{1}H NMR, (400 MHz, DMSO-d_6), δ 6.90 - 6.72 (m, 4H), 6.57 (dd, J = 16.8, 8.8 Hz, 4H), 6.34(s, 1H), 5.11 (s, 2H), 4.98 (s, 2H), 2.25 (s, 3H). ^{13}C NMR (100 MHz, DMSO-$d6$) δ 172.77, 171.41, 165.51, 147.12, 146.39, 143.33, 142.47, 122.32, 122.21, 114.91, 114.65, 100.25, 24.04. HRMS (APCI) m/z: $[M + H]^+$ calculated for $C_{17}H_{16}O_2N_4$, 309.1330; found, 309.1335.

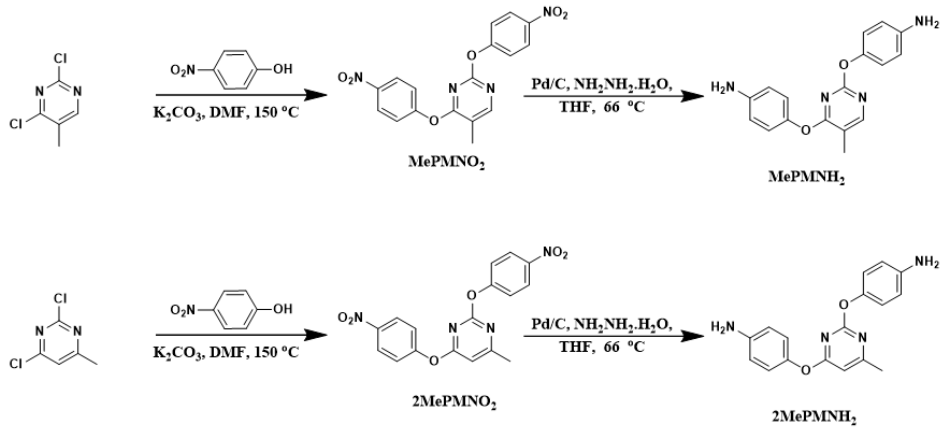

Scheme. S1. Synthesis of $MePMNH_2$ and $2MePMNH_2$.

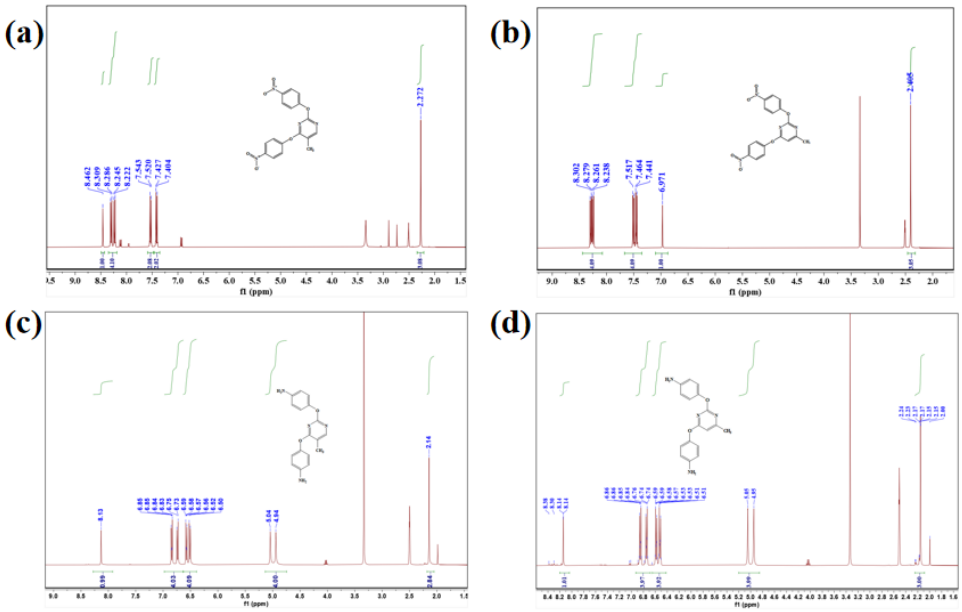

Fig. S1. ^{1}H NMR spectrum of (a) $MePMNO_2$, (b) $2MePMNO_2$, (c) $MePMNH_2$ and (d) $2MePMNH_2$ in DMSO-d6.

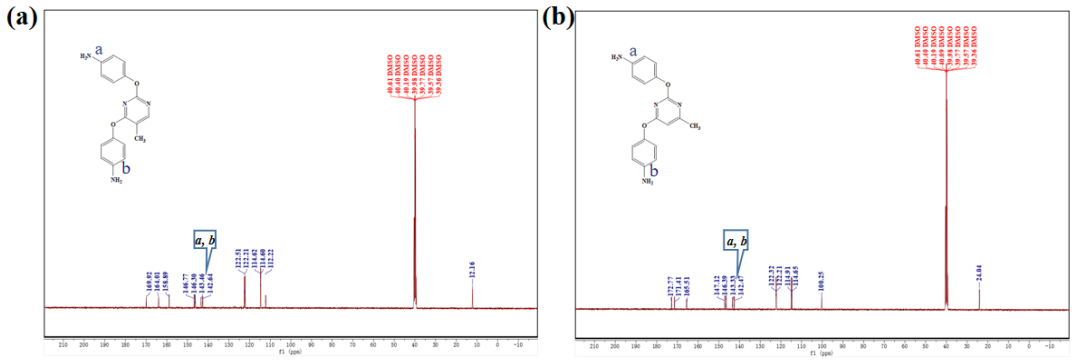

Fig. S2. ^{13}C NMR spectrum of (a) $MePMNH_2$ and (b) $2MePMNH_2$ in DMSO-d6.

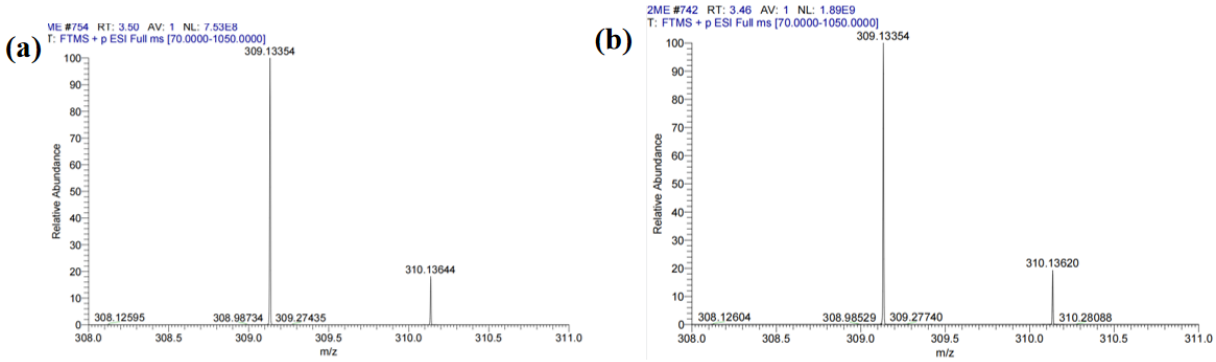

Fig. S3. HRMS spectrum of (a) $MePMNH_2$ and (b) $2MePMNH_2$.

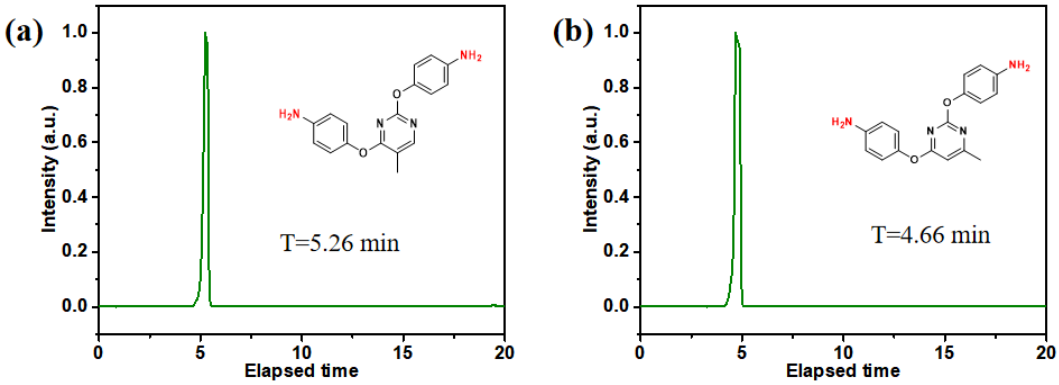

Fig. S4. HPLC spectrum of (a) $MePMNH_2$ and (b) $2MePMNH_2$.

III. Additional FTIR spectra and XRD patterns of PI films.

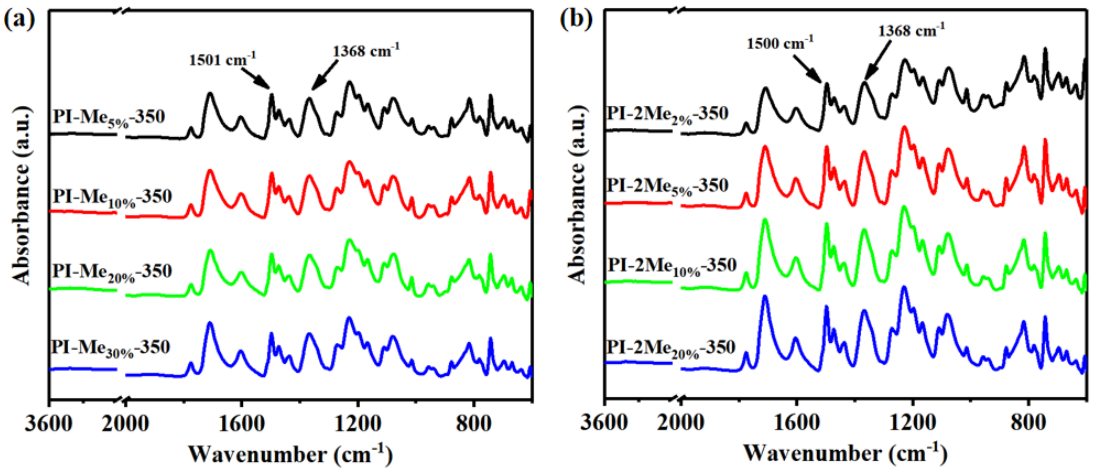

Fig. S5. FTIR spectra of (a) (MePMNH$_2$/ODA)/ODPA co-PI films and (b) (2MePMNH$_2$/ODA)/ODPA co-PI films.

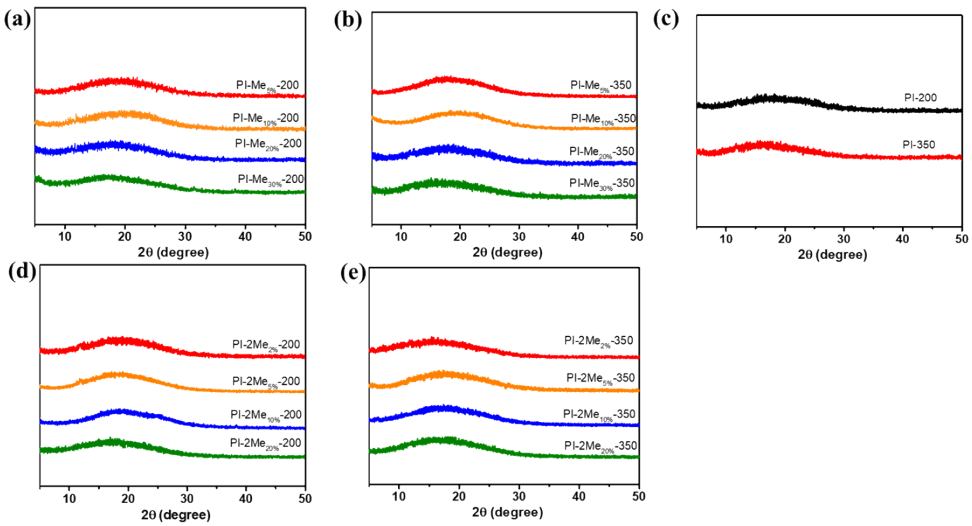

Fig. S6. XRD patterns of (a) (MePMNH$_2$/ODA)/ODPA co-PI films cured at 200°C, (b) (MePMNH$_2$/ODA)/ODPA co-PI films cured at 350°C; (c) (2MePMNH$_2$/ODA)/ODPA co-PI films cured at 200°C, (d) (2MePMNH$_2$/ODA)/ODPA co-PI films cured at 350°C; (e) ODA/ODPA PI films cured at 200°C and 350°C.

IV. Additional TMA curves and linearly polarized IR spectroscopy of PI films.

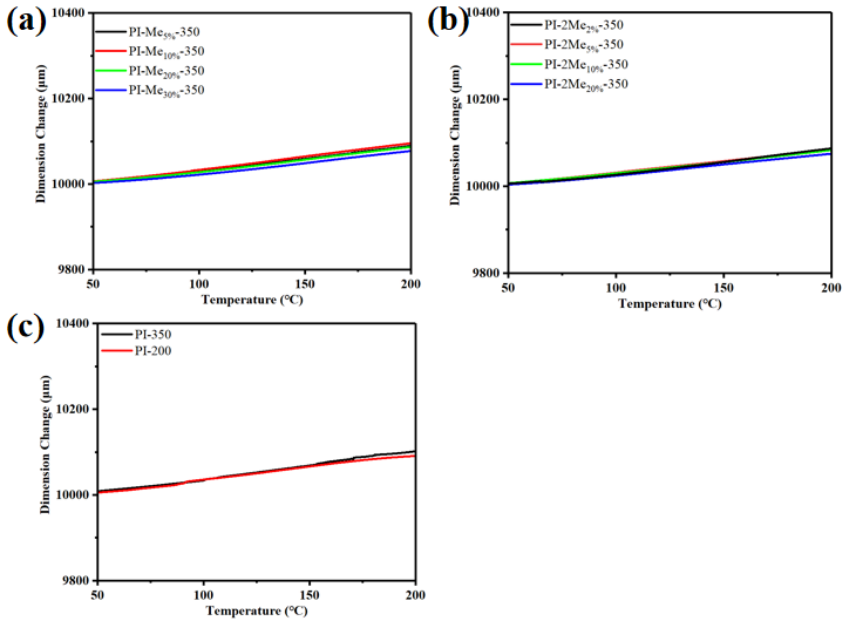

Fig. S7. TMA curves of (a) ($MePMNH_2$/ODA)/ODPA co-PI films, (b) ($2MePMNH_2$/ODA)/ODPA co-PI films and (c) ODA/ODPA PI films.

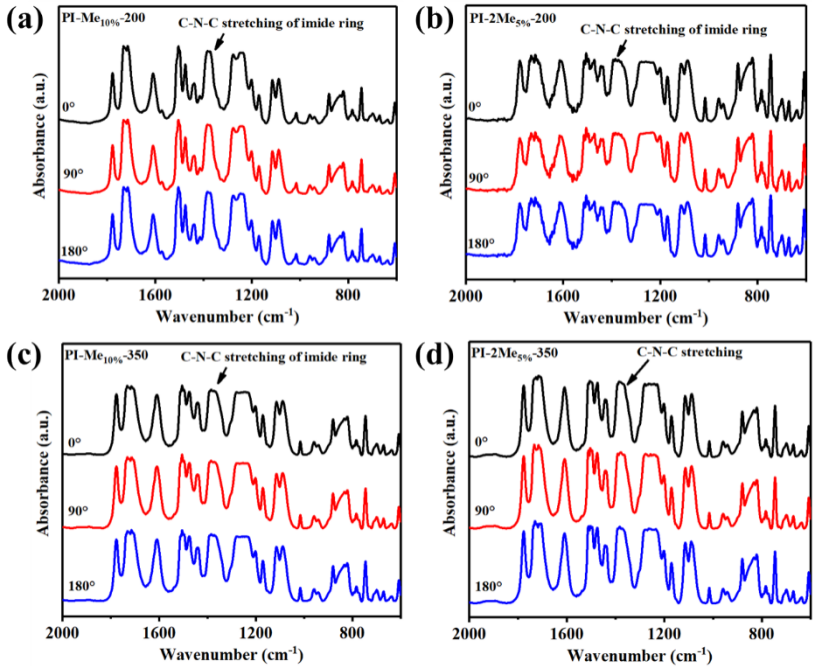

Fig. S8. Linearly polarized IR spectroscopy of (a) PI-$Me_{10\%}$-200, (b) PI-$2Me_{5\%}$-200, (c) PI-$Me_{10\%}$-200, (d) PI-$2Me_{5\%}$-350.

V. Additional TGA curves and stress–strain curves of PI films.

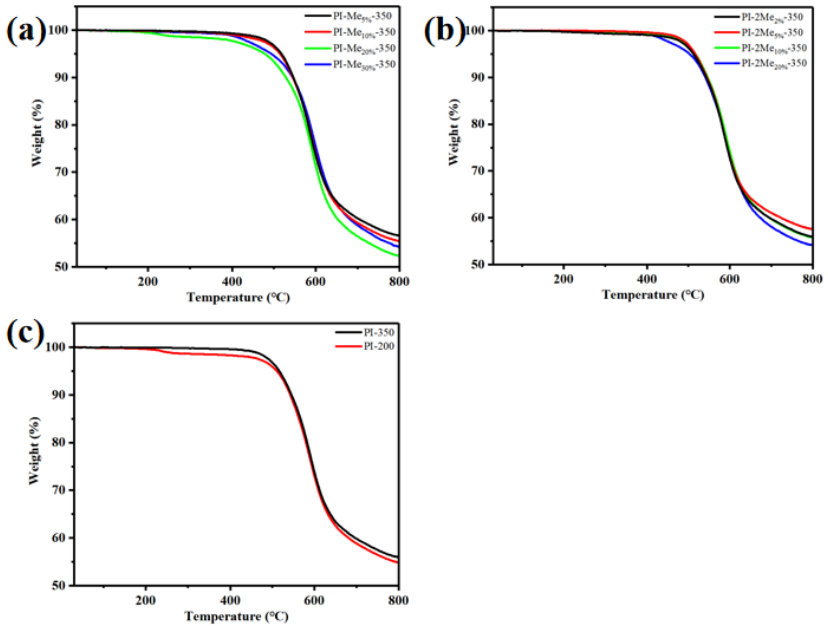

Fig. S9. TGA curves of (a) (MePMNH$_2$/ODA)/ODPA co-PI films, (b) (2MePMNH$_2$/ODA)/ODPA co-PI films and (c) ODA/ODPA PI films.

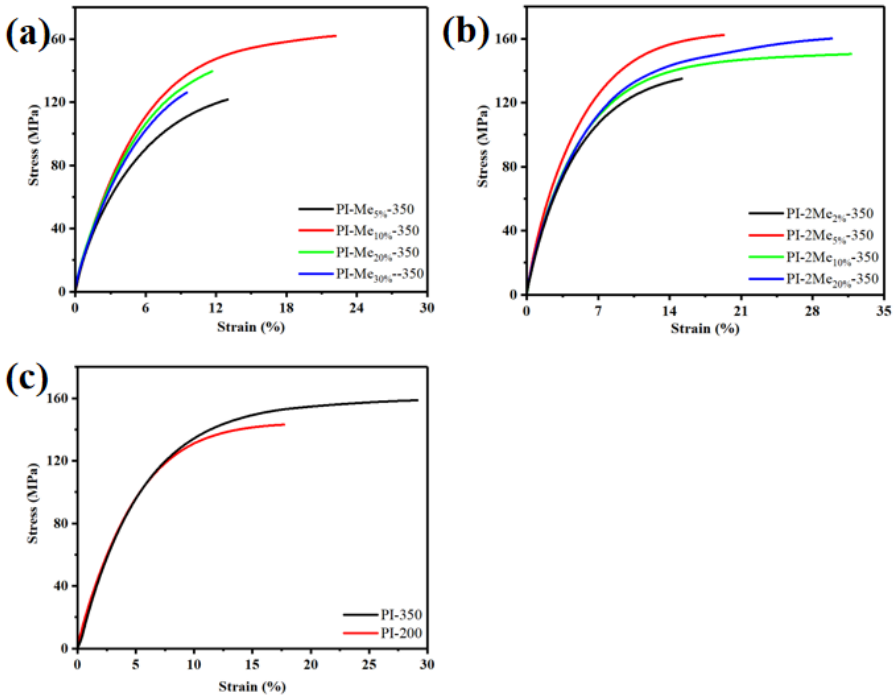

Fig. S10. Typical stress–strain curves of (a) (MePMNH$_2$/ODA)/ODPA co-PI films, (b) (2MePMNH$_2$/ODA)/ODPA co-PI films and (c) ODA/ODPA PI films.

VI. The cyclic voltammetry curves.

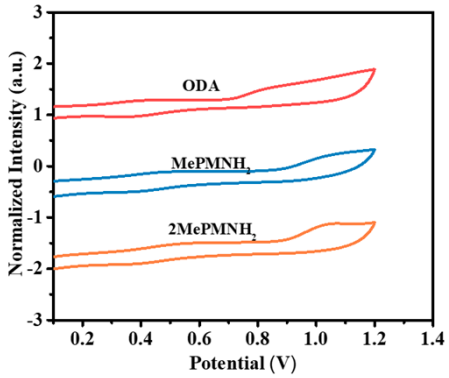

Fig. S11. The cyclic voltammetry curves of three diamines.

VII. UV–vis transmission spectra of co-PI films.

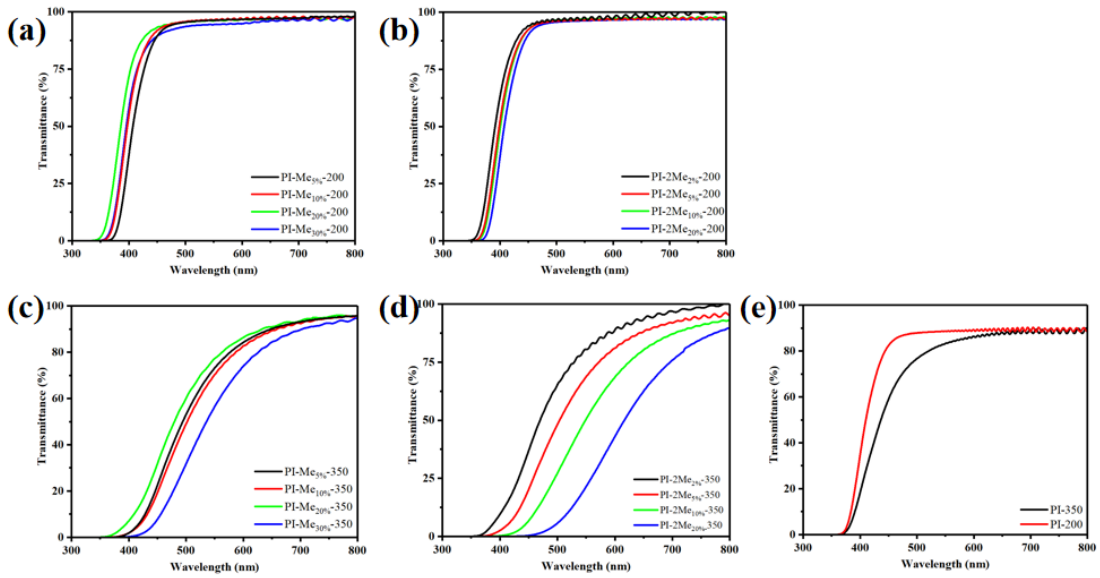

Fig. S12. UV–vis transmission spectra of (a) ($MePMNH_2$/ODA)/ODPA co-PI films cured at 200 °C, (b) ($2MePMNH_2$/ODA)/ODPA co-PI films cured at 200 °C, (c) ($MePMNH_2$/ODA)/ODPA co-PI films cured at 350 °C, (d) ($2MePMNH_2$/ODA)/ODPA co-PI films cured at 350 °C, and (e) ODA/ODPA PI films.

VIII. Additional detailed data of PI films.

Table S1. Detailed data of CTE and dichroic ratio of the resulting PI films cured at 350°C.

Sample Name	CTE (ppm/K)	Dichroic ratio	Diamine Ratio(n)
PI-350	68.33	2.09	ODA
PI-$Me_{5\%}$-350	55.57	2.02	ODA:$MePMNH_2$=0.5:9.5
PI-$Me_{10\%}$-350	59.48	2.07	ODA:$MePMNH_2$=1.0:9.0
PI-$Me_{20\%}$-350	54.25	2.17	ODA:$MePMNH_2$=2.0:8.0
PI-$Me_{30\%}$-350	49.86	2.18	ODA:$MePMNH_2$=3.0:7.0
PI-2$Me_{2\%}$-350	54.78	2.10	ODA:2$MePMNH_2$=0.2:9.8
PI-2$Me_{5\%}$-350	53.15	2.05	ODA:2$MePMNH_2$=0.5:9.5
PI-2$Me_{10\%}$-350	50.96	2.09	ODA:2$MePMNH_2$=1.0:9.0
PI-2$Me_{20\%}$-350	47.44	2.05	ODA:2$MePMNH_2$=2.0:8.0

Table S2 Solubility of the resulting PI films cured at 200°C in this study[a].

Sample Name	NMP	DMF	DMAc	DMSO	THF
PI-200	++−−	+−−−	+−−−	+−−−	−−−−
PI-$Me_{5\%}$-200	++−−	+−−−	+−−−	+−−−	−−−−
PI-$Me_{10\%}$-200	++−−	+−−−	+−−−	+−−−	−−−−
PI-$Me_{20\%}$-200	++++	+++−	+++−	+++−	−−−−
PI-$Me_{30\%}$-200	++++	+++−	+++−	+++−	−−−−
PI-2$Me_{2\%}$-200	++−−	+−−−	++−−	+−−−	−−−−
PI-2$Me_{5\%}$-200	++−−	+−−−	++−−	+−−−	−−−−
PI-2$Me_{10\%}$-200	++−−	+−−−	+−−−	+−−−	−−−−
PI-2$Me_{20\%}$-200	+++−	+++−	+++−	+−−−	−−−−

[a] ++++: soluble at room temperature; +++−: partially soluble at room temperature; ++−−: soluble by heating; +−−−: partially soluble by heating; and −−−−: insoluble by heating. Qualitative solubility was determined using 5 mg of PI film in 8 mL of solvent at room temperature.

Table S3. Mechanical and thermal properties of the resulting PI films cured at 350°C.

Sample Name	$T_{d5\%}$ (°C)	$T_{d10\%}$ (°C)	T_g (°C)	R_{800^oC} (°C)	E (GPa)	σ_{max} (MPa)	ε_b (%)
PI-350	516	545	264	54.93	2.89	159	29.1
PI-$Me_{5\%}$-350	513	545	272	56.59	3.12	122	13.0
PI-$Me_{10\%}$-350	515	545	287	55.45	3.13	162	22.2
PI-$Me_{20\%}$-350	479	529	302	52.28	3.32	140	11.7

PI-$Me_{30\%}$-350	494	544	305	54.02	3.47	126	9.5
PI-$2Me_{2\%}$-350	512	543	280	57.25	3.18	135	15.2
PI-$2Me_{5\%}$-350	516	545	280	57.56	4.09	162	19.1
PI-$2Me_{10\%}$-350	517	547	298	55.80	3.56	150	31.2
PI-$2Me_{20\%}$-350	503	541	306	54.07	3.85	160	29.1

Table S4. Dielectric properties of the resulting PI and commercial kapton film.

Sample Name	Dielectric constant (10 GHz)	Dielectric loss factors (10^{-2}) (10 GHz)
PI-350	3.24	1.20
PI-$Me_{5\%}$-350	3.08	1.11
PI-$Me_{10\%}$-350	3.04	1.06
PI-$Me_{20\%}$-350	3.33	1.50
PI-$Me_{30\%}$-350	3.49	1.73
PI-$2Me_{2\%}$-350	3.09	1.26
PI-$2Me_{5\%}$-350	3.27	0.92
PI-$2Me_{10\%}$-350	3.42	1.12
PI-$2Me_{20\%}$-350	3.52	1.32
PI-200	3.30	1.44
PI-$Me_{5\%}$-200	3.23	1.38
PI-$Me_{10\%}$-200	3.00	1.11
PI-$Me_{20\%}$-200	3.13	0.89
PI-$Me_{30\%}$-200	3.42	1.23
PI-$2Me_{2\%}$-200	3.18	1.26
PI-$2Me_{5\%}$-200	3.38	1.26
PI-$2Me_{10\%}$-200	3.40	1.18
PI-$2Me_{20\%}$-200	3.47	1.23
kapton film	3.41	1.57

Table S5. The performance of reported low temperature curable PI films.

Ref	Thermal properties		Mechanical properties			Electrical properties		Curing conditions		
	T_g	$T_{d,5\%}$	σ_{max}	ε_b	E	D_k	D_f	T_c	Accelerator	Dosage
	[℃]	[℃]	[MPa]	[%]	[GPa]	(10 GHZ)	(10 GHZ)	[℃]		
6	271	543	89	5.5	2.21	-	-	320	-	-
7	225	510	-	-	-	-	-	220	QL	700%
8	289	592	112	75.5	1.27	-	-	200	QL	200%
9	428	526	91	15	6.34	3.36	-	200	A-BZI	4.14%
10	271	551	109	7.0	3.3	-	-	200	-	-
10	291	546	122	8.6	3.5	-	-	200	-	-

11	376	576	148	98.49	1.66	-	-	200	QL	150%
12	-	480	-	-	-	-	-	280	Et_3N	66.7%
1	-	545	134.82	145.16	1.66	3.36	2.89%	200	QL	150%
1	-	456	105.40	45.37	1.01	3.46	3.23%	200	IQL	150%
13	281	-	-	-	-	-	-	160	-	-
14	272	546.1	-	-	-	-	-	300	-	-
15	292	558	150	14.3	3.1	-	-	200	-	-
This work	230	455	151	8.2	3.83	3.13	0.89%	200	-	-
This work	246	515	163	21.1	4.13	3.38	1.26%	200	-	-

References

1 C. Huang, J. Li, D. Sun, R. Xuan, Y. Sui, T. Li, L. Shang, G. Zhang, R. Sun and C. P. Wong, *Journal of Materials Chemistry C*, 2020, **8**, 14886-14894.

2 C. Pu, D. Lin, H. Xu, F. Liu, H. Gao, G. Tian, S. Qi and D. Wu, *Polymer,* 2022, **255,** 125119.

3 V.M. Svetlichnyi, N.G. Antonov, B.V. Chernitsa, V.M. Denisov, A.I. Koltsov, V.V. Kudryavtsev and M.M. Koton, *Vysokomolekulyarnye Soedineniya Seriya A*, 1986, **28**, 2412-2418.

4 F. Weigend and R. Ahlrichs, *Physical Chemistry Chemical Physics*, 2005, **7**, 3297-3305.

5 C.T. Lee and W.T. Yang, *Physical Review B*, 1988, **37**, 785-789.

6 J.O. Simpson and A.K. St Clair, *Thin Solid Films*, 1997, **308**, 480-485.

7 R. Lian, X. Lei, Y. Chen and Q. Zhang, *Journal of Applied Polymer Science,* 2019, **136**, 47771.

8 Y. Ding, B. Bikson and J.K. Nelson, *Macromolecules*, 2002, **35**, 905-911.

9 Y. Sui, J. Li, T. Wang, D. Sun, C. Huang, F. Zhang, L. Shan, F. Niu, G. Zhang and

R. Sun, *Polymer*, 2021, **218**, 123514.

10 C. Li, Y. Wang, Y. Yin, Y. Li, J. Li, D. Sun, J. Lu, G. Zhang and R. Sun, *Polymer*, 2021, **228**, 123963.

11 C. Huang, J. Li, G. Zhang and R. Sun, *Macromolecular Materials and Engineering*, 2019, **304**, 1900505.

12 W.-H. Liao, S.-Y. Yang, S.-T. Hsiao, Y.-S. Wang, S.-M. Li, C.-C.M. Ma, H.-W. Tien and S.- J. Zeng, *ACS Appl. Mater. Interfaces*, 2014, **6**, 15802–15812.

13 X. Han, Y. Tian, L. Wang, C. Xiao and B. Liu, *European Polymer Journal*, 2007, **43**, 4382-4388.

14 X. Liu, X.W. Cao, G.J. He and T.C. Xing, *Express Polymer Letters*, 2019, **13**, 524-532.

15 C. Li, G. Zhang, J. Li and Y. Sui, *International Conference on Electronic Packaging Technology*, 2021.